Novel actuation design of a gait trainer with shadow leg approach

Jos Meuleman
Moog Robotics
Nieuw-Vennep, The Netherlands
jmeuleman@moog.com

Jos Meuleman, Edwin H.F. van Asseldonk, Herman van der Kooij
Department of Biomechanical Engineering
University of Twente
Enschede, The Netherlands

***Abstract*— Robotic gait training has developed since the end of the 20th century, yet there is much room for improvement in the design of the robots. With the conventional exoskeleton structures, donning of patients in a gait trainer usually is a cumbersome process due to the need of joint alignments and normal walking is often hindered due to obstructed arm swing. Our goal was to design a gait training robots that overcomes these limitations. We propose a novel design in which these drawbacks are reduced to a great amount. By using a parallel structure behind the patient (shadow leg) that is connected to the patient joints with rods, little alignment is needed, the area lateral to the hip is left free, and thus arm swing is not obstructed. The construction is lightweight, because the actuators are mounted on a fixed base and the transmission of power is executed with light weight rods. An end stop in the shadow leg prevents hyper extension of the patient's knee. The relationship between motor displacement and human joint rotations is non-linear. In this paper we derive the nonlinear relationships between motors and patient joints and verify these. calculations with a measurement.. The device has been built, now tests with subjects are required to assess if subjects can indeed walk normally in the robot.**

Keywords—robotic gait trainer; locomation; admittance control; shadow leg; rods; exoskeleton

I. INTRODUCTION

Since the end of the 20th century numerous gait training robots have been developed. The robots enhanced the understanding of the underlying mechanism of human gait and pathological gait. The newly acquired knowledge and the existing knowledge in rehabilitation led to several robots that replace the strenuous physical labor of physiotherapists [1], [2]. After a few years of putting the gait training robots in practice, the first evaluation results were published. Until now robot-aided gait training has not led to results superior to conventional training [3–5]. The existing gait training robots require improvements on several aspects.

The latest insights in efficient gait training are that gait training robots should provide assistance only when needed [6]. This requires robots to allow free motion of the patient, with the robot following the patient's motions without hindering. This requires force controlled robots [7], [8].

A second limitation of current gait training robots is that installation of the patient (donning) often requires 10 to 20 minutes, which is a considerable fraction compared to the duration of training sessions (30-60 minutes) This drawback seriously hinders the acceptance of gait training robots in rehabilitation centers. The long donning time can be ascribed to the fact that most gait training robots use numerous straps and require alignment of the exoskeleton with the patient [1], [2], [9]. If misalignment between the patient joint and mechanical joint occurs (e.g. by difference in geometry), this results in high, uncomfortable forces on the patient. Therefore the alignment of the robot leg to the patient leg is critical, but it is a time consuming process.

Finally normal walking in current gait training robots is difficult, if not impossible. Natural arm swing is often hindered, since most gait training robots have an exoskeleton located lateral to the hips of the patient. Additionally, most gait training robots allow motion in a limited number of degrees of freedom (DoFs) and restrict motion in other DoFs that show considerable motion during normal walking. This inhibits normal walking, and thus proper implementation of Assist As Needed and transfer of the learned walking abilities in the robot to over ground walking.

We propose a novel design that overcomes these limitations: a shadow leg that is located behind the

This study was supported by a grant from Dutch Ministry of Economic affairs and Province of Overijssel, the Netherlands (grant: PID082004)

978-1-4673-6024-1/13/$31.00 ©2013 IEEE

patient and attaches to the patient by means of rods. This is incorporated in the design of Lopes II. With conventional exoskeletons the kinematic relationship between motor and patient joint is straightforward, with the parallel structure of the shadow leg, the kinematics are non-linear and contain cross couplings. This paper addresses the rationale and kinematic model of the design of the shadow leg.

II. GLOBAL DESIGN DESCRIPTION

A. *Fixed base actuation*

Regardless the control strategy, it is important to design a lightweight structure for the gait training robot. The dynamic mass of the structure should be kept as low as possible. The location of the actuators is crucial in this. By placing the actuators on a fixed base, the moving mass can be kept low.

B. *Power transfer options*

The next step is to provide the proper gearing method to transfer the power from the actuator to the subject. A common approach is to link each actuator to a joint. For fixed based actuation there are only a few transmissions possible. Lopes I uses a Bowden cable mechanism [10], but suffers from wear and has a limited bandwidth. Noël used an electrohydraulic transmission [11] but hydraulics tend to leak. Therefore we selected the approach of push-pull rods, linking the actuators to the rotation of the segment instead of segments.

C. *Shadow leg*

To transfer the torques to the segments we use a shadow leg approach [12]. which is a mechanical leg behind the patient that is connected to the actuators. Each shadow leg is connected to the patient by three rods. One rod connecting the patient hip to the shadow hip, a second rod connecting the patient knee to the shadow knee, a third rod connecting the patient ankle to the shadow ankle.

This offers three main advantages. The first is that contrary to the lateral exoskeletons, the shadow leg does not hinder arm-swing. Second, no exact alignment of the shadow leg with the patient is required – only rough alignment of the knee and hip joint and third the end-stop for knee hyperextension can be built in the shadow leg.

The rod that points towards the hip is connected to a pelvis strap that is integrated in a harness. There is no material to the side of the pelvis other than the belt of the harness. Thus arm swing is possible. It is

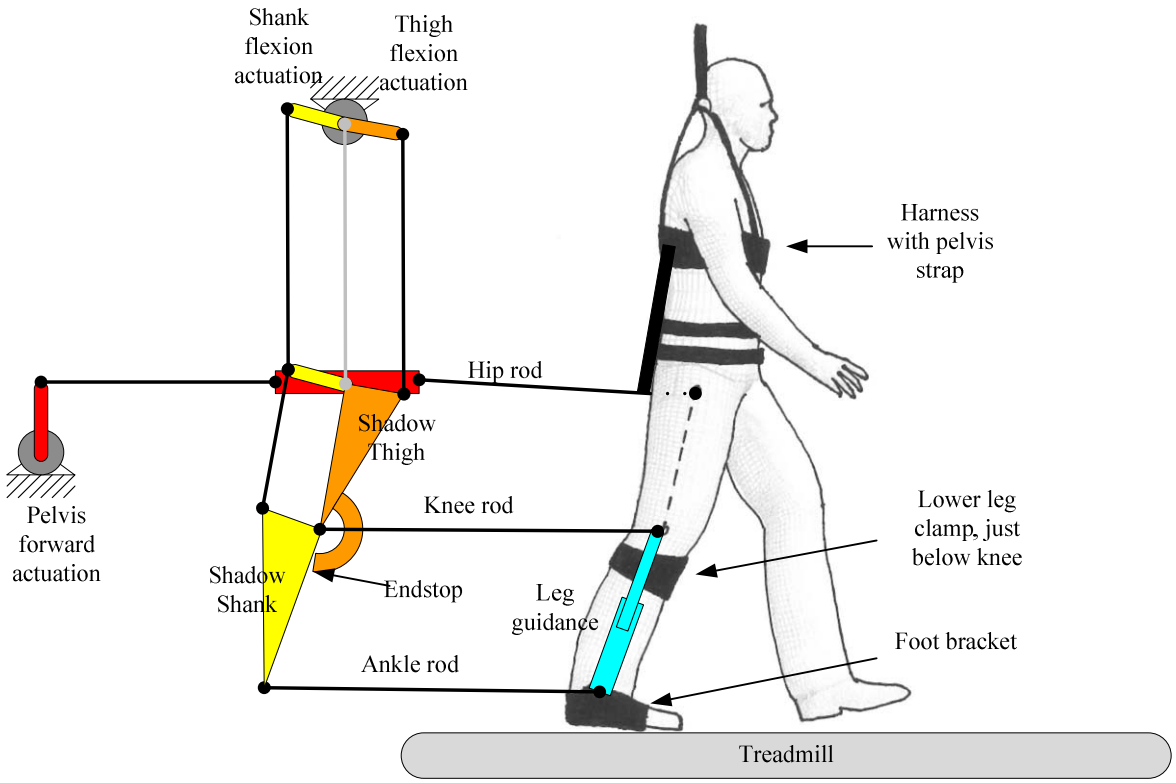

Fig. 1. Layout of the Lopes II gait training robot.

important that the hip rod point towards the patient hip, and not higher to the back. If forces were applied on the back instead of on the hip, a force to stretch a leg caused an uncomfortable bending moment on the spine, pushing a subject into a hollow back.

The knee rod points towards the patient knee. By simple prototypes we discovered that a clamp just below the knee is the best place to apply the force pointing to the knee. This place allows for a relatively stiff connection, with acceptable comfort. An extra prerequisite however is that the force on the clamp is exerted perpendicular to the leg. Any tangential component will cause the knee clamp to slide. We used a leg guidance that runs parallel to the subject's leg and is connected to the knee rod and the ankle rod (Fig. 1.). The knee clamp slides along leg guidance. A negative side effect from using this guidance is that it requires an extra adjustment of the length of the guidance to assure that the knee rod points towards the knee.

The rod pointing towards the ankle is connected to a foot bracket, by means of a spherical gimbal [13] which has the center of rotation in the ankle joint. This assures that the forces from the ankle rod are exerted on the ankle without imposing torques on the foot. Also the spherical gimbal allows for limited inversion and endorotation.

Abduction is applied by applying abduction to the shadow leg, the ankle rod then pulls the foot outward. The shadow hip is attached to a stage that is actuated in the horizontal plane, this way pelvis horizontal forces are applied to the patient.

D. *Admittance control*

To assure that the patient can walk normally, the robot should display minimal impedance, i.e. it should feel very light for the patient. Two factors are important here: the real mass of the moving parts of the robot and the used control strategy. With control, a significant portion of the moving mass can be reduced. We chose admittance control [14], [15] for the Lopes II since this offers a large dynamic bandwidth, i.e. both low and high impedance. With admittance control the perceived mass of the moving parts can be reduced. According to Colgate this is limited to a factor of two [16] , when passivity is obeyed, but in the HapticMASTER the virtual mass is reduced by a factor of ten [17], maintaining passivity with human interaction. Nonetheless it is important to design the mechanics with minimal moving mass. To implement admittance control, force sensors are required, preferably as close to the patient as possible.

III. KINEMATICS OF THE SHADOW LEG

For the control it is needed to have the relationship between the patient joint angles ($X_{patient}$) and the motor angles (X_{motor}). Due to the geometry this transformation is nonlinear. Also this transformation depends on the limb size of the patient ($L_{patient}$) (1). This transformation is split into the transformation from patient- to shadow leg angles (2a) and the transformation from shadow leg angles to motor angles.

$$X_{motor} = F(X_{patient}, L_{patient}) \quad (1)$$

$$X_{shadowleg} = F_2(X_{patient}, L_{patient}) \quad (2a)$$

$$X_{motor} = F_1(X_{shadowleg}); \quad (2b)$$

The transformation from shadow leg angle to motor angle is straightforward and therefore not discussed in this paper. The transformation from patient leg to shadow leg is a more complicated transformation since it depends on the patient limb size. For the control and design of the shadow leg it is important to know what the range of motion of the shadow leg must be. Additionally the calculations are used to verify that the end stop on the shadow knee extension can be used as an end stop for the patient knee extension.

A. *Geometry*

The targeted population of the Lopes II ranges from subjects of 1.41 m stature (Dined, Dutch 2004 (60 plus), female mu-3sigma) to 2.088 m stature (Dined, : Dutch 2004 (20-30 years), male mu+3sigma). For the shank and thigh length we used stature multiplied by a factor as given by Winter [18] (see TABLE I.).

TABLE I. DIMENSIONS OF PATIENT LIMBS AND SHADOW LEG

	Subject		Shadow leg
	Min	***Max***	
Stature [mm]	1410	2088	
Shank Length [mm]	347	514	450
Thigh Length [mm]	345	512	450

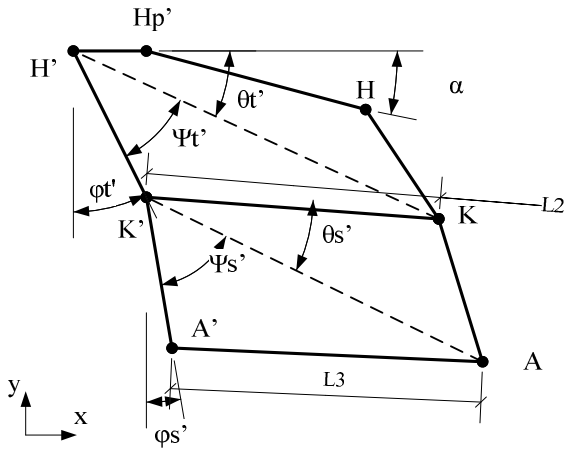

Fig. 2. Patient leg (H-K-S) connected to the shadow leg (H'-K'-A')

Fig. 2. shows the patient's leg, consisting of hip (H), knee (K) and ankle (A), and the shadow leg defined by shadow hip (H'), shadow knee (K') and shadow ankle (A'). The length of the shadow thigh ($L_{T'}$) and shadow shank ($L_{S'}$) are set to 0.45 m. The rod from the shadow ankle to the patient ankle is one meter (L_s). The rod from the shadow knee to the patient knee is adjustable in length, approximately one meter (L_2). The patient's hip is connected to a point (Hp') located near the shadow hip (H'). Ideally Hp' and H' coincide, but, since the shadow hip is a mechanically complex joint, the hip rod is connected to Hp'. The distance |H-Hp'| is 0.8 meter and the distance |Hp'-H'| is 0.2 meter.

$$L_{T'} = |K'H'| \tag{3}$$

$$L_{S'} = |A'K'| \tag{4}$$

B. kinematic model

With a given patient posture (joint angles and pelvis location), the shadow leg angles can be calculated. This is the inverse kinematics (2a). We now derive the kinematics assuming a rigid structure.

Assume that the patient's hip (H), knee (K) and ankle (A) joint coordinates are given. The vertical coordinate of the shadow hip (H') is determined by the structure. Then the horizontal coordinate is determined by the rods H-Hp' and Hp'-H'.

To calculate the shadow thigh angle $(\varphi_t)_{'}$, we first calculate the vector from the shadow hip to the patient knee K-H' (dotted line in Fig.2.)

Converting this vector to polar coordinates gives a length ($L_{KH'}$) and an angle ψ_0

$$L_{KH'} = |KH'| \tag{5}$$

$$\theta_{t'} = \tan^{-1}(KH'_y / KH'_x) \tag{6}$$

Now we solve the triangle H'-K'-K, by using the cosine rule

$$L_2^2 = L_{KH'}^2 + L_{T'}^2 - 2\, L_{KH'}\, L_{T'} \cos(\psi_{t'}) \tag{7}$$

$$\psi_{t'} = \pm\cos^{-1}\left[(L_{KH'}^2 + L_{T'}^2 - L_2^2)/ 2\, L_{KH'}\, L_{T'}\right] \tag{8}$$

Note that the solution for this (5) delivers a positive and negative angle. The angle should be selected that results in a shadow thigh angle that is closest to the patient thigh angle. The thigh flexion can be defined as:

$$\varphi_{t'} = \pi - \theta_{t'} - \psi_{t'} \tag{9}$$

Analogously the shank flexion is calculated

$$L_{AK} = |AK'| \tag{10}$$

$$\psi_{s'0} = \tan^{-1}(AK'_y / AK'_x) \tag{11}$$

$$\psi_{s'} = \cos^{-1}\left[(L_{AK}^2 + L_{S'}^2 - L_3^2)/ 2\, L_{AK}\, L_{S'}\right] \tag{12}$$

$$\varphi_{s'} = \pi - \psi_{s'0} - \psi_{s'} \tag{13}$$

Finally the shadow hip angle is equal to the shadow thigh angle and the shadow knee angle is the shadow thigh angle minus the shadow shank angle (14).

$$\varphi_{h'} = \varphi_{t'} \tag{14a}$$

$$\varphi_{k'} = \varphi_{t'} - \varphi_{s'} \tag{14b}$$

Similarly the forward kinematics i.e. the calculation from shadow joint angles, to patient joint angles can be calculated.

C. Straight leg calculations

A physical end stop is implemented on the shadow knee to prevent hyperextension of the

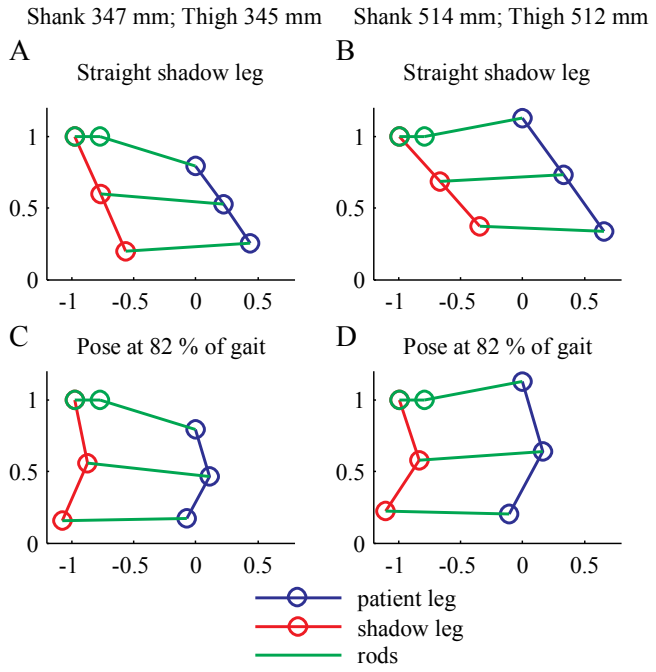

Fig. 3. Various configurations of patient attached to the shadow leg. The shortest patient with straight leg swung forward (A), with a normal gait pattern (C). The tallest person with straight leg swung forward (B), with a normal gait pattern (D)

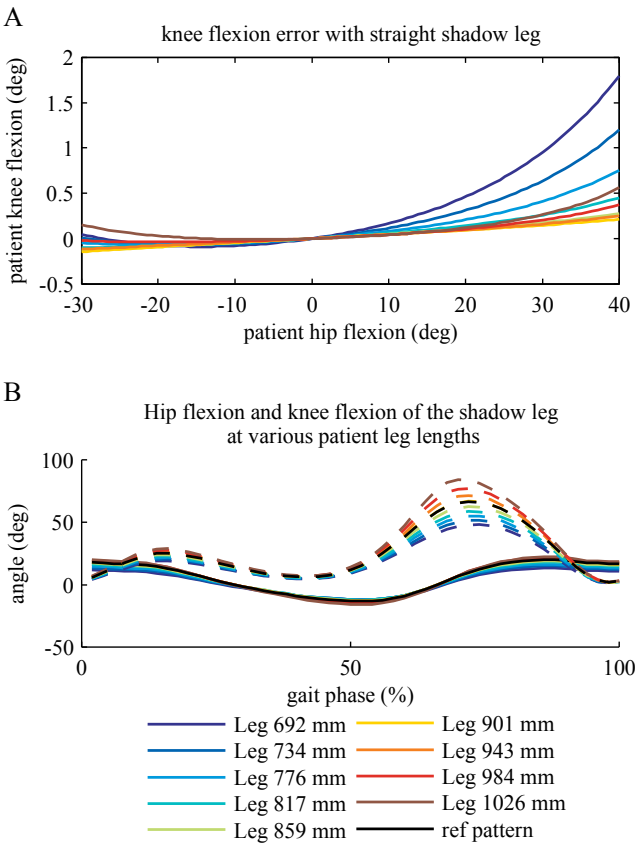

Fig. 4. A: patient knee flexion when the leg is swung and the shadow leg knee is kept zero. B: angles of the shadow leg for normal gait, solid line is the shadow hip angle, the dashed line is the shadow knee angle. The black lines are the referance patterns for hip and knee

patient knee (negative flexion). As derived above, the relation depends on patient size and rod lengths. The rod to the knee is adjustable in length to assure that in stance the end stop of the shadow knee coincides with the maximum allowable extension of the knee. This way, hyperextension of the knee in mid stance is prevented, but since the relation between shadow joints and patient joints is nonlinear, we need to calculate the patient knee angle when a straight patient leg (with the shadow knee locked) is swung along the full range of the hip. This is done in the next section.

D. Numerical examples

We performed numerical computations for the shortest and tallest subject, to assess the required range of motion of the shadow leg and to test if the end stop on the shadow knee extension does not allow hyperextension of the patient knee. We used joint angles from Winter [19] for normal cadence to calculate the shadow joint angles (see Fig 3.C and D and Fig.4.B.) For the shortest patient, the shadow angles are smaller than the patient angles, for the tallest patient the shadow angles are larger than the patient angles (see Fig. 4.B).

Additionally we locked the shadow knee (end stop reached), swung the patient hip from 30 degrees extension to 40 degrees extension. Fig. 3 shows the configurations for the shortest leg (A) and the longest leg (B). We calculated the patient knee flexion (see Fig. 4A). The maximum knee extension is 0.2 degrees. When the hip is flexed to 40 degrees, for both the shortest and tallest subject, the knee is flexed for less than one degree.

IV. IMPLEMENTATION

A. Design

The geometry as calculated above is used in the detailing of the design of the shadow leg. Based on the gait data the required range of motion of the shadow leg is calculated. Similarly the torques on the segments are calculated. And thus the required strength of the components is calculated.

The final design of the shadow leg is given in Fig. 5. The shadow leg is designed such that for all sizes of patients as defined in TABLE I. The patient hip ranges from 30 degrees extension to 40 degrees

flexion and the knee ranges from zero to 75 degrees flexion.

In this paper abduction of the shadow leg and patient leg is not discussed, though it is implemented already in the design of the shadow leg as discussed above. To apply abduction the rods to the ankle and hip must be stiff in lateral direction, therefore they are built as an A-frame. The shadow leg must be torsional stiff, therefore the upper and lower leg are built with tubular shapes.

The force sensors for the control loop are located close to the patient. The only inertias that are perceived by the patient are that of the components that are between the patient and the force sensor and the virtual inertia that is displayed by the control loop.

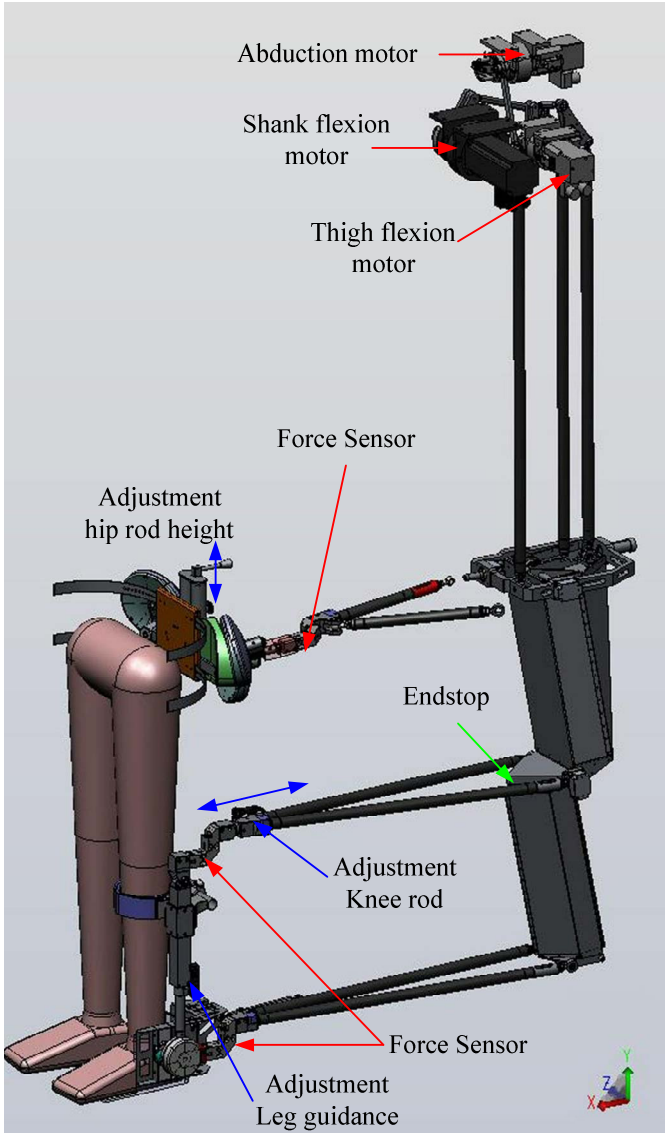

Fig. 5. Design of the shadow leg and the actuation

B. *Implementation and operation*

Fig.5. shows a CAD drawing of the shadow leg as was built for the Lopes II. To don a patient in the Lopes the leg guidance of the Lopes is set to the proper shank length and the length of the knee rod is adjusted to make sure that the hyper extension end stop on the shadow knee coincides with maximum extension of the patient knee. The height of the hip rods should be adjusted to make sure that the hip rods are point to the hip joints.

V. PRELIMINARY RESULTS

We implemented the kinematic model in a real time controller (RTAI, 2048 Hz) We used a test dummy equipped with a hip and knee joint (see Fig. 7.). We commanded a knee and hip pattern that resembles walking to test if our kinematic model is

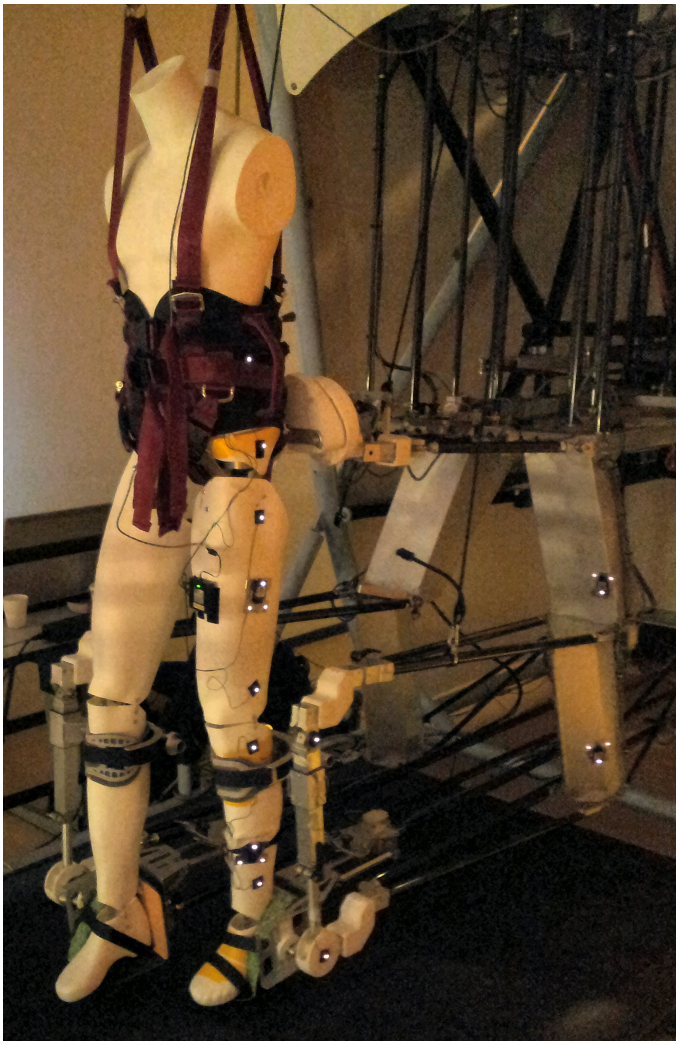

Fig. 6. Dummy equipped with markers strapped in the Lopes

accurate in controlling a desired gait pattern. With an optical tracking system (Visualeyez VZ4000, PTI, Burnaby, Canada) we measured the shank and thigh orientation of the dummy in the sagittal plane. We recorded the measured positions and the commanded segment orientation

The measured and desired angles are close to each other (see Fig.7). The root mean square error (RMSE) of the thigh is 1.17 degrees; the RMSE for the shank error is 1.62 degrees.

A resonance frequency is visible on the measured shank angle, due to an undesired compliance in the used setup, indicating that our assumption of a rigid structure is not fully justified. Another cause of errors could be the minor play and compliance of the clamps and the difference between real linkage dimensions and dimensions that are used in the kinematics.

The stiffness will be increased and linkage dimensions will be checked to increase the accuracy. Finally compliance can be modeled in the kinematics to increase the accuracy.

VI. Conclusion & Discussion

In the design of the Lopes II we focused on normal walking and quick donning and doffing. The shadow leg configuration reduces the need of alignment and adjustment. The only remaining alignment and adjustment in the Lopes II are the length of the knee rod, length adjustment of the leg guidance and alignment of the harness, such that the hip rods are pointing to the hip joints. The area lateral to the hips is absent from mechanics and thus arm swing is unhindered.

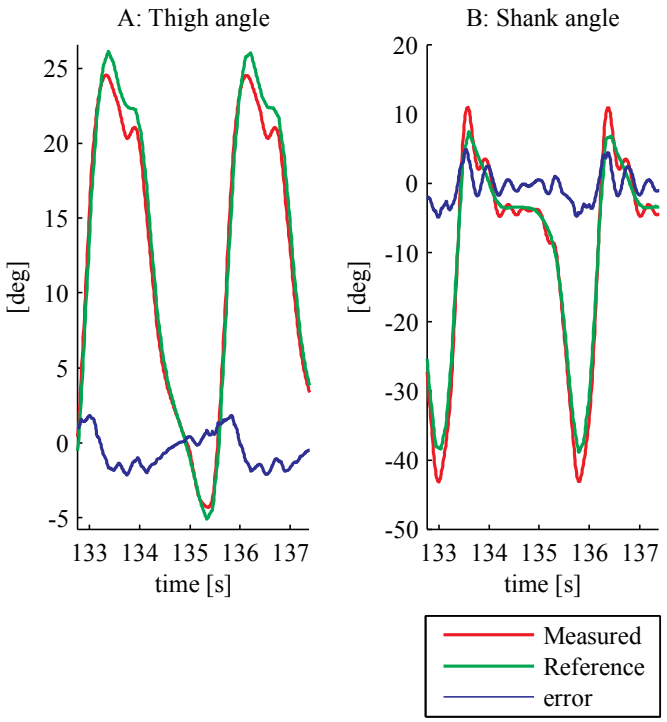

Fig.7.The thigh angle (A), as measured, as commaned, and the error. The shank angle (B), as measured, as commanded and the error/

Preliminary results show that the non-linear kinematic model can used in a real time controller resulting in minor errors (<2deg) in the segment orientation. Further development of the model and the robot should increase the accuracy of the kinematic model. Subsequently, we will verify that walking is unhindered by the device in a population of healthy subjects and neurological patients.

References

[1] G. Colombo, M. Joerg, R. Schreier, and V. Dietz, "Treadmill training of paraplegic patients using a robotic orthosis," *J Rehabil Res Dev*, vol. 37, no. 6, pp. 693–700, 2000.

[2] S. Hesse, D. Uhlenbrock, and T. Sarkodie-Gyan, "Gait pattern of severely disabled hemiparetic subjects on a new controlled gait trainer as compared to assisted treadmill walking with partial body weight support.," 1999.

[3] B. Husemann, F. Muller, C. Krewer, S. Heller, and E. Koenig, "Effects of locomotion training with assistance of a robot-driven gait orthosis in hemiparetic patients after stroke: a randomized controlled pilot study," *Stroke*, vol. 38, no. 2, pp. 349–354, 2007.

[4] S. Banala, S. Kim, S. Agrawal, and J. Scholz, "Robot assisted gait training with active leg exoskeleton (ALEX)," *IEEE transactions on neural systems and rehabilitation engineering*, vol. 17, no. 1, pp. 2–8, 2009.

[5] J. Hidler, D. Nichols, M. Pelliccio, K. Brady, D. Campbell, J. Kahn, and T. Hornby, "Multicenter randomized clinical trial evaluating the effectiveness of the lokomat in subacute stroke," *Neurorehabil Neural Repair*, vol. 23, no. 1, pp. 5–13, 2009.

[6] M. D. Ziegler, H. Zhong, R. R. Roy, and V. R. Edgerton, "Why variability facilitates spinal learning.," *The Journal of neuroscience□: the official journal of the Society for Neuroscience*, vol. 30, no. 32, pp. 10720–6, Aug. 2010.

[7] E. H. F. van Asseldonk, J. F. Veneman, R. Ekkelenkamp, J. H. Buurke, F. C. T. van der Helm, H. van der Kooij, E. H. F. Van Asseldonk, and F. C. T. Van Der Helm, "The Effects on Kinematics and Muscle Activity of Walking in a Robotic Gait Trainer During Zero-Force Control.," *IEEE transactions on neural systems and rehabilitation engineering□: a publication of the IEEE Engineering in Medicine and Biology Society*, vol. 16, no. 4, pp. 360–370, Aug. 2008.

[8] H. Vallery, A. Duschau-wicke, and R. Riener, "Generalized Elasticities Improve Patient-Cooperative Control of Rehabilitation Robots," pp. 535–541, 2009.

[9] J. F. Veneman, R. Kruidhof, E. E. G. Hekman, R. Ekkelenkamp, E. H. F. Van Asseldonk, and H. van der Kooij, “Design and evaluation of the LOPES exoskeleton robot for interactive gait rehabilitation.,” *IEEE transactions on neural systems and rehabilitation engineering□: a publication of the IEEE Engineering in Medicine and Biology Society*, vol. 15, no. 3, pp. 379–86, Sep. 2007.

[10] J. F. Veneman, R. Ekkelenkamp, R. Kruidhof, F. C. T. van der Helm, and H. van der Kooij, “Design of a series elastic- and Bowden cable-based actuation system for use as torque-actuator in exoskeleton-type training,” in *Rehabilitation Robotics, 2005. ICORR 2005. 9th International Conference on*, 2005, pp. 496–499.

[11] M. Noel, B. Cantin, S. Lambert, C. M. Gosselin, and L. J. Bouyer, “An electrohydraulic actuated ankle foot orthosis to generate force fields and to test proprioceptive reflexes during human walking,” *IEEE Trans Neural Syst Rehabil Eng*, vol. 16, no. 4, pp. 390–399, 2008.

[12] J. H. Meuleman, “Rehabilitation apparatus,” U.S. Patent UK Patent Application 1222322.8; International Patent Application PCT/EP2013/0533542013.

[13] J. H. Meuleman, “Mechanical spherical linkage,” U.S. Patent UK Patent Application Number 1305989.4; right to file international patent applications reserved2013.

[14] R. Q. Van Der Linde and P. Lammertse, “HapticMaster – a generic force controlled robot for human interaction,” *Industrial Robot An International Journal*, vol. 30, no. 6, pp. 515–524, 2003.

[15] J. A. Maples and J. J. Becker, “Experiments in force control of robotic manipulators,” *Robotics and Automation. Proceedings.*, vol. 3, pp. 695–702, 1986.

[16] E. Colgate and N. Hogan, “An analysis of contact instability in terms of passive physical equivalents,” in *Robotics and Automation 1989 Proceedings 1989 IEEE International Conference on*, 1989, no. Piscataway, NJ, United States, pp. 404–409.

[17] J. Osnabrugge, “Analysis of an Admittance Controlled Haptic Display during Contact Situations,” Control Laboratory, University of Twente, 2001.

[18] D. A. Winter, “Biomechanics and Motor Control of Human Movement.” Nueva York, EUA□: Wiley, 1990.

[19] D. A. Winter, *The biomechanics and motor control of human gait*. University of Waterloo Press, 1987.